

This discussion paper is/has been under review for the journal Biogeosciences (BG).
Please refer to the corresponding final paper in BG if available.

Projections of ocean acidification over the next three centuries using a simple global climate carbon-cycle model

C. A. Hartin, B. Bond-Lamberty, P. Patel, and A. Mundra

Pacific Northwest National Laboratory, Joint Global Change Research Institute at the University of Maryland–College Park, 5825 University Research Court, College Park, MD 20740, USA

Received: 15 October 2015 – Accepted: 23 November 2015 – Published: 4 December 2015

Correspondence to: C. A. Hartin (corinne.hartin@pnnl.gov)

Published by Copernicus Publications on behalf of the European Geosciences Union.

BGD

12, 19269–19305, 2015

Projections of ocean acidification over the next three centuries

C. A. Hartin et al.

Title Page

Abstract

Introduction

Conclusions

References

Tables

Figures

◀

▶

◀

▶

Back

Close

Full Screen / Esc

Printer-friendly Version

Interactive Discussion



Abstract

Continued oceanic uptake of anthropogenic CO₂ is projected to significantly alter the chemistry of the upper oceans, potentially having serious consequences for the marine ecosystems. Projections of ocean acidification are primarily determined from prescribed emission pathways within large scale earth system models. Rather than running the cumbersome earth system models, we can use a reduced-form model to quickly emulate the CMIP5 models for projection studies under arbitrary emission pathways and for uncertainty analyses of the marine carbonate system. In this study we highlight the capability of Hector v1.1, a reduced-form model, to project changes in the upper ocean carbonate system over the next three centuries. Hector is run under historical emissions and a high emissions scenario (Representative Concentration Pathway 8.5), comparing its output to observations and CMIP5 models that contain ocean biogeochemical cycles. Ocean acidification changes are already taking place, with significant changes projected to occur over the next 300 years. We project a low latitude ($> 55^\circ$) surface ocean pH decrease from preindustrial conditions by 0.4 units to 7.77 at 2100, and an additional 0.27 units to 7.50 at 2300. Aragonite saturations decrease by 1.85 units to 2.21 at 2100 and an additional 0.80 units to 1.42 at 2300. Under a high emissions scenario, for every 1 °C of future warming we find a 0.107 unit pH decrease and a 0.438 unit decrease in aragonite saturations. Hector reproduces the global historical trends, and future projections with equivalent rates of change over time compared to observations and CMIP5 models. Hector is a robust tool that can be used for quick ocean acidification projections, accurately emulating large scale climate models under multiple emission pathways.

BGD

12, 19269–19305, 2015

Projections of ocean acidification over the next three centuries

C. A. Hartin et al.

Title Page	
Abstract	Introduction
Conclusions	References
Tables	Figures
◀	▶
◀	▶
Back	Close
Full Screen / Esc	
Printer-friendly Version	
Interactive Discussion	



1 Introduction

Human induced activities have led to increasing anthropogenic emissions of greenhouse gases to the atmosphere. In the first decade of the 21st century CO₂ emissions from anthropogenic sources and land use changes accounted for ~ 9 PgCyr⁻¹, with future emission projections of up to 28 PgCyr⁻¹ by 2100 under a high emissions scenario (RCP 8.5) (Riahi et al., 2011). In response to this increasing atmospheric burden of CO₂, the oceans are experiencing both physical and biogeochemical changes: surface and deep warming, changes in calcium carbonate saturations, and a decline in pH (Doney, 2010). The oceans represent a major carbon sink and have absorbed 25–30 % of the total anthropogenic carbon emissions since 1750 (Le Quéré et al., 2013; Sabine et al., 2011). There is some concern due to both the physical and chemical changes that the oceans will be less efficient in the uptake of anthropogenic CO₂ as the climate continues to change (Sarmiento and Le Quéré, 1996; Matear and Hirst, 1999; Joos et al., 1999; Le Quéré et al., 2007, 2010).

In particular, the ocean chemistry is quickly changing in response to the continued addition of CO₂ to the atmosphere. Mean surface ocean pH has decreased by 0.1 units relative to the preindustrial (Caldeira et al., 2003). If emission trends continue, ocean acidification will occur at rates and extents that have not been observed over the last few million years (Feely et al., 2004, 2009; Kump et al., 2009; Caldeira et al., 2003). Ocean acidification occurs when CO₂ dissolves in seawater, forming H₂CO₃, dissociating to H⁺ and HCO₃⁻. The H⁺ ions quickly react with CO₃²⁻ forming more bicarbonate. The net effect of adding CO₂ to the system increases the concentration of H₂CO₃, HCO₃⁻ and H⁺, while decreasing CO₃²⁻ concentrations and lowering the pH, acting to inhibit further uptake of CO₂. HCO₃⁻, CO₃²⁻ and CO₂ (aq), make up the total dissolved inorganic carbon (DIC). A doubling of CO₂ will not cause a corresponding doubling of CO₂ (aq) but instead will result in an increase of ~ 10 % in the oceans, due to the nonlinearity of the carbonate system and buffering capacity of the oceans. At a pH of

[Title Page](#)[Abstract](#)[Introduction](#)[Conclusions](#)[References](#)[Tables](#)[Figures](#)[◀](#)[▶](#)[◀](#)[▶](#)[Back](#)[Close](#)[Full Screen / Esc](#)[Printer-friendly Version](#)[Interactive Discussion](#)

8.2, 88 % of the DIC is in the form of HCO_3^- , 11 % in the form of CO_3^{2-} , and 0.5 % in the form of CO_2 (aq), these percentages will change as the oceans take up more carbon.

With declining CO_3^{2-} , the stability of biogenic carbonate (CaCO_3) is also reduced which is the primary mineral used by marine organisms to build their shells and skeletons. Numerous experiments and observations indicate that a reduction in the surface ocean pH and carbonate saturations may have significant effects on calcifying marine organisms, e.g., phytoplankton and coral reefs, from changes in community structure to suppressed calcification rates (Feely et al., 2004; Riebesell et al., 2000; Fabry et al., 2008; Kleypas et al., 2005; Raven et al., 2005; Dutkiewicz et al., 2015). For example, some coral reefs are believed to already be eroding for parts of the year due to changes in ocean acidification (Yates and Halley, 2006; Albright et al., 2013). Modeling studies project changes in ocean acidification for both the surface and deep oceans. By the end of the century all existing coral reefs will be surrounded by ocean chemistry conditions that are well outside of the preindustrial values and even today's saturations (Ricke et al., 2013). Global surface pH is projected to drop by up to 0.4 units under IS92a scenario and even deep waters will experience pH changes of up to 0.3 units by 2100 under RCP8.5 (Gehlen et al., 2014; Orr et al., 2005). Ocean warming and acidification are consistent across all of the CMIP5 models, however the intensities are strongly dependent upon the scenario (Bopp et al., 2013). These studies indicate that the oceans are already experiencing and will continue to experience significant changes in ocean acidification.

However, these model projections of ocean acidification are primarily from earth system models (ESMs) run under prescribed emission pathways (e.g., RCPs); limiting the analyses that can be conducted to only those scenarios. Here we present Hector, a reduced-form climate model that can emulate the median climate of CMIP5. Reduced-form models are powerful tools due to their computational efficiency, inexpensiveness to run, and ability to run multiple simulations under arbitrary future climate change emission pathways, allowing us to conduct parameter sensitivity studies

Projections of ocean acidification over the next three centuries

C. A. Hartin et al.

[Title Page](#)

[Abstract](#)

[Introduction](#)

[Conclusions](#)

[References](#)

[Tables](#)

[Figures](#)



[Back](#)

[Close](#)

[Full Screen / Esc](#)

[Printer-friendly Version](#)

[Interactive Discussion](#)



and uncertainty analyses (Senior and Mitchell, 2000; Ricciuto et al., 2008; Irvine et al., 2012).

This study builds upon Hartin et al. (2015), which introduced Hector v1.0, an open-source, object-oriented simple climate model with the capabilities of projecting changes in the surface ocean carbonate system over the next three centuries. This work is timely due to the fact that the recent CMIP5 process included numerous ESMs that contain dynamic ocean biogeochemistry.

Other simple models have modeled the complexity of the nonlinear carbonate system through mixed layer Impulse Response Functions (IRF) calculating air-sea fluxes (Joos et al., 1996, 2001; Meinshausen et al., 2011) and evaluating the parameters of the carbonate system by back calculating from the ocean uptake of CO₂ (Tanaka et al., 2007; Harman et al., 2011). The IRF method has been widely used across the scientific community, as it is cost-effective to run, provides surface to deep mixing estimates, and can also be used to look at oceanic uptake of conservative tracers. However, the carbonate system is not directly calculated and many effects like temperature effects on CO₂ solubility are typically parameterized. The carbonate system is strongly dependent upon temperature where $p\text{CO}_2$ changes by about 4.2 % per Kelvin (Copin-Montegut, 1988; Takahashi et al., 1993). While these models are able to reproduce changes in the global climate system, details in the carbonate system (HCO_3^{2-} , CO₃, pH, $p\text{CO}_2$, and alkalinity) are not actively solved for.

The remainder of the paper is organized as follows. Section 2 describes the model components focusing on the ocean carbon cycle and carbonate chemistry. Section 3 presents the model experiments and comparison data used and lastly, Sect. 4 describes the main results and a discussion.

2 Model description – carbon cycle

The carbon component in Hector contains three carbon reservoirs: a single well-mixed atmosphere, a land component consisting of vegetation, detritus, and soil, and an

BGD

12, 19269–19305, 2015

Projections of ocean acidification over the next three centuries

C. A. Hartin et al.

[Title Page](#)

[Abstract](#)

[Introduction](#)

[Conclusions](#)

[References](#)

[Tables](#)

[Figures](#)

◀

▶

◀

▶

[Back](#)

[Close](#)

[Full Screen / Esc](#)

[Printer-friendly Version](#)

[Interactive Discussion](#)



Title Page	
Abstract	Introduction
Conclusions	References
Tables Figures	
◀	▶
◀	▶
Back	Close
Full Screen / Esc	
Printer-friendly Version	
Interactive Discussion	

ocean component consisting of four boxes (high and low surface boxes, an intermediate box, and a deep box) (Fig. 1). The change in atmospheric carbon is a function of the anthropogenic emissions (F_A), land-use change emissions (F_{LC}), and atmosphere–ocean (F_O) and atmosphere–land (F_L) carbon fluxes. The default model time step is 5 1 year.

$$\frac{dC_{atm}(t)}{dt} = F_A(t) + F_{LC}(t) - F_O(t) - F_L(t) \quad (1)$$

The terrestrial cycle in Hector contains vegetation, detritus, and soil, all linked to each other and the atmosphere by first-order differential equations. Vegetation net primary production is a function of atmospheric CO₂ and temperature. Carbon flows from the 10 vegetation to detritus and to soil and loses fractions of carbon to heterotrophic respiration on the way. An “earth” pool debits carbon emitted as anthropogenic emissions, allowing a continual mass-balance check across the entire carbon cycle. Atmosphere–land fluxes at time t are calculated by:

$$F_L(t) = \sum_{i=1}^n NPP_i(t) - RH_i(t) \quad (2)$$

15 where NPP is the net primary production and RH is the heterotrophic respiration summed over user-specified n groups (i.e., latitude bands, political units, or biomes) (Hartin et al., 2015).

3 Ocean component

The ocean component is modeled after Lenton (2000), Knox and McElroy (1984) and Sarmiento and Toggweiler (1984) consisting of four boxes; two surface boxes (high and low latitude), an intermediate and deep box, simulated a simple thermocline circulation. The cold high latitude surface box makes up 15 % of the ocean, representing 20

Title Page	
Abstract	Introduction
Conclusions	References
Tables	Figures
◀	▶
◀	▶
Back	Close
Full Screen / Esc	
Printer-friendly Version	
Interactive Discussion	

the subpolar gyres ($> 55^\circ$), while the warm low latitude surface box makes up 85 % of the ocean. The temperatures of the surface boxes are linearly related to the global atmospheric temperature change, and are initialized at 2 °C in the high latitude and 22 °C for the low latitude box. This temperature gradient sets up a flux of carbon into the cold high latitude box and a flux out of the warm low latitude box. The ocean–atmosphere flux of carbon is the sum of all the surface fluxes ($F_i = 2$).

$$F_O(t) = \sum_{i=1}^n F_i(t) \quad (3)$$

Once carbon enters the system it is circulated between the boxes via advection and water mass exchange, simulating a simple thermohaline circulation. We do not explicitly model diffusion. Simple box-diffusion models and “HILDA” (e.g., Siegenthaler and Joos, 1992) type models, are typically in good agreement with observations but are more computationally demanding than a simple box model (Lenton, 2000). The change in carbon of any box i is given by the fluxes in and out, with $F_{\text{atm}\rightarrow i}$ as the atmospheric carbon flux:

$$\frac{dC_i}{dt} = \sum_{j=1}^{\text{in}} F_{j\rightarrow i} - \sum_{j=1}^{\text{out}} F_{i\rightarrow j} + F_{\text{atm}\rightarrow i} \quad (4)$$

More specifically, the change in carbon of box i is related to the transport ($T_{i\rightarrow j}$) in Sverdrups ($\text{Sv} - \text{m}^3 \text{s}^{-1}$) between i and j , the volume of i (V_i), and the total carbon in i (including any air–sea fluxes) (C_i):

$$\frac{dC_i}{dt} = \frac{T_{i\rightarrow j}}{V_i} \times C_i \quad (5)$$

Volume transports are tuned to yield an approximate flow of 100 Pg C from the surface high latitude to the deep ocean at steady state, simulating deep water formation. The

dynamics of ocean uptake of CO₂ is strongly dependent on this downward transport rate of CO₂ laden waters from the surface ocean to depth.

There are 4 measurable parameters of the carbonate system in seawater: DIC, TA, pCO₂ and pH, and any pair can be used to describe the entire carbonate system.
5 Within Hector, DIC and TA are used to solve for surface ocean pH and pCO₂ values. These detailed carbonate chemistry equations are based on numeric programs from Zeebe and Wolf-Gladrow, 2001 (A). We have simplified these equations by neglecting the effects of pressure, since we are only concerned with the surface ocean. A best-fit alkalinity (2311.0 mol kg⁻¹ for HL and 2435.0 mol kg⁻¹ for LL), is solved for at the end
10 of spinup, that when calculated with an initial DIC input for each surface box results in a pre-industrial net zero flux of carbon over the global ocean. Hector is run to equilibrium in a perturbation-free mode, prior to running the historical period, ensuring that Hector is in steady-state (Hartin et al., 2015; Pietsch and Hasenauer, 2006). The alkalinity values are within the range of open ocean observations, 2250.0–2450.0 mol kg⁻¹
15 of solution (Key et al., 2004) and are held constant with time in Hector. We assume negligible carbonate precipitation/dissolution or alkalinity runoff from the land surface over our period of interest (100–300 years). From this, Hector actively solves for pCO₂, pH (total scale), and HCO₃⁻, CO₃²⁻, and aragonite (Ω_{Ar}) and calcite saturations (Ω_{Ca}) in the surface ocean boxes.

20 pCO₂ is calculated from the concentration of [CO₂^{*}] and the solubility of CO₂ in seawater, based on salinity, temperature, and pressure. [CO₂^{*}] is calculated from DIC and the first and second dissociation constants of carbonic acid from Mehrbach et al. (1973), refit by Lueker et al. (2000) (A1). pCO₂ is needed to calculate atmosphere ocean carbon fluxes (Takahashi et al., 2009):

$$25 F = k\alpha \times \Delta p\text{CO}_2 = \text{Tr} \times \Delta p\text{CO}_2 \quad (6)$$

where k is the CO₂ gas-transfer velocity, α is the solubility of CO₂ in seawater (K_0), and the $\Delta p\text{CO}_2$ is the difference in [CO₂] between the atmosphere and ocean. The product of k and α results in Tr, the sea-air gas transfer coefficient, where Tr (gCm⁻²

BGD

12, 19269–19305, 2015

Projections of ocean acidification over the next three centuries

C. A. Hartin et al.

[Title Page](#)

[Abstract](#)

[Introduction](#)

[Conclusions](#)

[References](#)

[Tables](#)

[Figures](#)



[Back](#)

[Close](#)

[Full Screen / Esc](#)

[Printer-friendly Version](#)

[Interactive Discussion](#)



month⁻¹ μ atm⁻¹) = 0.585 · α · Sc^{-1/2} · U₁₀², 0.585 is a unit conversion factor and Sc is the Schmidt number (A1) is calculated from Wanninkhof (1992) based on the temperature of each surface box. The average wind speed (U_{10}) of 6.7 m s⁻¹ is the same over both surface boxes (Table 1). We assume surface waters are fully equilibrated with the overlying atmosphere given our time step of 1 year; the average time for surface waters to come into equilibrium (Broecker and Peng, 1982). pH (total scale), HCO₃⁻, and CO₃²⁻ are calculated using the H⁺ ion, solved for in a higher order polynomial (A1).

Aragonite and calcite are the two primary carbonate minerals within seawater. The degree of saturation in seawater with respect to calcite (Ω_{Ca}) and aragonite (Ω_{Ar}) is calculated from the product of the concentrations of calcium [Ca²⁺] and carbonate ions [CO₃²⁻], divided by the solubility (K_{sp}). The calcium concentration is based on equations from Riley and Tongudai (1967) at a constant salinity of 35. If $\Omega = 1$, the solution is at equilibrium, and if $\Omega > 1$ ($\Omega < 1$) the solution is supersaturated (undersaturated) with respect to the mineral.

$$\Omega = \frac{[\text{Ca}^{2+}][\text{CO}_3^{2-}]}{K_{\text{sp}}} \quad (7)$$

4 Model experiments and data sources

The Hector code is open-source and available at <https://github.com/JGCRI/hector>. The repository includes all model code needed to compile, as well as, all input files and R scripts to process the model output. For this study we run Hector v1.1, Git Commit #, with updated ocean temperature to better match the CMIP5 mean. Hector is run under prescribed emissions from 1850–2300 for all four Representative Concentration Pathways (RCP 2.6, RCP 4.5, RCP 6, RCP 8.5) (Moss et al., 2010; Fujino et al., 2006; van Vuuren et al., 2007; Clarke et al., 2007; Wise et al., 2009; Riahi et al.,

Title Page	Abstract	Introduction
Conclusions	References	
Tables	Figures	
◀	▶	
◀	▶	
Back	Close	
Full Screen / Esc		
Printer-friendly Version		
Interactive Discussion		



2007; Hijioka et al., 2008; Smith and Wigley, 2006). All emissions data is available at <http://tntcat.iiasa.ac.at/RcpDb/>.

Comparison data is obtained from a series of observational surface data and a suite of CMIP5 models. Surface ocean observations of DIC, $p\text{CO}_2$, pH, Ω_{Ar} , and Ω_{Ca} are from ocean time-series stations in both the high and latitude oceans; Hawaii Ocean Time Series (HOT), Bermuda Atlantic Time Series (BATS), the European Station for Time Series in the Ocean at the Canary Islands (ESTOC), the Irminger Sea, and the Iceland Sea (Table 3) (Bates, 2007; Fujieki et al., 2013; Dore et al., 2009; Santana-Casiano et al., 2007; Olafsson, 2007a, b; Gonzalez-Davila, 2009). The time-series data are annually averaged over the upper 100 m of the water column. The carbonate parameters not found in Table 3 are computed from temperature, salinity, and carbonate parameter pairs using the CO2SYS software (Lewis and Wallace, 1998). Lastly, a longer record (1708–1988) of pH and Ω_{Ar} from Flinder's Reef in the western Coral Sea is used in the comparison (Pelejero et al., 2005). We use rates of change (Δ) over a 20 year period (1991–2011) to quantify how well Hector does at simulating the observed changes in the ocean carbonate parameters.

We also compare Hector to a suite of 15 CMIP5 Earth System Models (Table 4) (Taylor et al., 2012). The CMIP5 output is available from the Program for Climate Model Diagnostics and Intercomparison (<http://cmip-pcmdi.llnl.gov/cmip5/>). The CMIP5 data are converted to annual global, high latitude and low latitude averages over the upper 100 m of water depth, with one standard deviation of the annual averages and CMIP5 model range calculated using the RCMIP5 package (<https://github.com/JGCRI/RCMIP5>). All CMIP5 comparisons used in this study are from model runs with prescribed atmospheric concentrations. We acknowledge that this is not a perfect comparison between emissions forced Hector and concentration forced CMIP5. However, very few CMIP5 models were run under prescribed emissions. We use a combination of root mean square error (RMSE) and rates of change (Δ) as our metrics to characterize how well Hector compares to the CMIP5 median.

12, 19269–19305, 2015

BGD

Projections of ocean acidification over the next three centuries

C. A. Hartin et al.

[Title Page](#)

[Abstract](#)

[Introduction](#)

[Conclusions](#)

[References](#)

[Tables](#)

[Figures](#)

◀

▶

◀

▶

[Back](#)

[Close](#)

[Full Screen / Esc](#)

[Printer-friendly Version](#)

[Interactive Discussion](#)



5 Results and Discussion

Hartin et al. (2015) conducted a thorough analysis of Hector v1.0 demonstrating how it can reproduce the historical trends and future projections of atmospheric [CO₂], radiative forcing, and global temperature under the RCPs. For this discussion we focus on the upper ocean high and low latitude inorganic carbon chemistry under RCP 8.5, comparing to a suite of earth system models included in the CMIP5 archive and observations. Hector's primary carbonate parameter outputs are summarized in Table 5. Figures 2–6 compare Hector to observations and CMIP5 median, one standard deviation and model spread.

DIC and $p\text{CO}_2$, functions of the inorganic carbon species in seawater, are directly related to rising temperatures and atmospheric [CO₂]. Hector captures the trend in DIC concentrations for both the high and low latitude surface ocean with an average RMSE of 4.6 $\mu\text{mol kg}^{-1}$ when compared to CMIP5 models over the historical period (Fig. 2). Low latitude DIC is slightly higher than the CMIP5 range, but rates of change are similar between 1850 and 2100, 1.27 yr^{-1} for Hector and 1.24 yr^{-1} for CMIP5 (Table 5). To obtain a steady state, Hector is initialized with carbon values slightly higher than the average CMIP5 values. Hector accurately tracks the $p\text{CO}_2$ in both the high and low latitude surface ocean with similar rates of change from 1850–2300 (Fig. 3). There is a low bias in Hector compared to CMIP5 models after 2100, highlighted by the higher RMSE; 1.4 μatm between 2006–2100 increasing to 6.0 μatm between 2006–2300. This is due to the low bias in projected atmospheric [CO₂] over the same time period (Hartin et al., 2015).

The oceanic uptake of CO₂ since the preindustrial has caused the marine carbonate system to shift to lower pH and lower [CO₃²⁻]. Hector accurately captures the decline in pH compared to CMIP5 and observations from BATS, HOT, ESTOC, Irminger Sea, Iceland Sea, and Flinders Reef (Fig. 4). Since the pre-industrial, surface ocean pH decreased by 0.08 units, corresponding to a 24% increase in [H⁺] concentrations and an 8% decrease in [CO₃²⁻]. This is in close agreement with numerous studies (Feely

BGD

12, 19269–19305, 2015

Projections of ocean acidification over the next three centuries

C. A. Hartin et al.

[Title Page](#)

[Abstract](#)

[Introduction](#)

[Conclusions](#)

[References](#)

[Tables](#)

[Figures](#)

◀

▶

◀

▶

[Back](#)

[Close](#)

[Full Screen / Esc](#)

[Printer-friendly Version](#)

[Interactive Discussion](#)



Projections of ocean acidification over the next three centuries

C. A. Hartin et al.

[Title Page](#)

[Abstract](#)

[Introduction](#)

[Conclusions](#)

[References](#)

[Tables](#)

[Figures](#)

◀

▶

◀

▶

[Back](#)

[Close](#)

[Full Screen / Esc](#)

[Printer-friendly Version](#)

[Interactive Discussion](#)



et al., 2004; Sabine et al., 2004; Caldeira et al., 2003; Orr et al., 2005) that estimate an average global decrease in pH of 0.1 or a 30 % increase in H⁺. The Flinder's Reef pH record provides a natural baseline to compare future trends in ocean acidification. While we don't expect to match exactly, as this reef site is heavily influenced by coastal dynamics, internal variability, and upwelling, rates of change from the pre-industrial (1750) to 1988 are the same (0.0002 yr⁻¹) for both Hector and Flinder's Reef (Table 5). Over the limited observational record from both the Pacific and Atlantic Oceans (1992–2006), Hector accurately simulates the change in pH (−0.0015 yr⁻¹) compared to BATS (−0.0018 yr⁻¹), HOT (−0.0014 yr⁻¹), ESTOC (−0.0017 yr⁻¹) and CMIP5 (−0.0017 yr⁻¹). More observations in the North Pacific show surface changes of pH of up to 0.06 units between 1991 and 2006 with an average rate of −0.0017 yr⁻¹ (Byrne et al., 2010). Rates of change in high latitude pH over the same time period are −0.0018 yr⁻¹ for Hector and CMIP5. Under RCP 8.5, Hector projects a decrease of over 0.40 units to 7.77 from 1850 to 2100 and by over 0.6 units to 7.5 by 2300 in low latitude ocean pH, similar to CMIP5 (Table 5) and findings from intermediate complexity models (Montenegro et al., 2007). At approximately 2050, atmospheric [CO₂] is double the pre-industrial concentrations, corresponding to a 0.20 pH decrease to 7.96. Shortly after this doubling, pH values are well outside the lowest observed natural variability found in Flinder's Reef.

Aragonite and calcite are forms of biogenic calcium carbonate. Foraminifera and coccolithophorids are composed of calcite the less soluble form of biogenic calcium carbonate, while corals and pteropods are composed of aragonite. Hector accurately simulates the decline in saturations (Ω_{Ar} and Ω_{Ca}) from 1850–2300 under RCP8.5 to CMIP5 and observations (Fig. 5). Since the preindustrial, surface low (high) latitude Ω_{Ar} decreased by 0.4 (0.3) units, with similar rates for CMIP5. Rates of change over a 14 year period for Hector (−0.007 yr⁻¹) agree well with CMIP5 (−0.006 yr⁻¹) and HOT (−0.010 yr⁻¹). Repeat oceanographic surveys in the Pacific Ocean observed an average 0.34 % yr⁻¹ decrease in the saturation state of surface seawater with respect

to aragonite and calcite over a 14 year period (1991–2005) (Feely et al., 2012), while the average decrease in Hector is between 19 and 25 %.

Saturations Of both Ar and Ca decrease rapidly over the next 100 years in both the high and low latitude. Hector accurately captures the decline in saturations with low RMSE values for both Ω_{Ar} (0.027) and Ω_{Ca} (0.012). Under RCP8.5 Hector projects that low latitude Ω_{Ar} will decrease by 1.85 units to 2.21 by 2100 and by 2.6 units to 1.42 by 2300. For low latitude Ω_{Ca} , Hector projects low latitude Ω_{Ca} decrease by 2.88 units to 3.34 by 2100 and by over 4.09 units to 2.31 by 2300. A lowering of Ω_{Ar} from approximately 4 to 3 is predicated to lead to significant reductions in calcification rates in tropical reefs (Kleypas et al., 1999; Silverman et al., 2009). In agreement with Roy et al. (2015) and Ricke et al. (2013) by the end of the 21st century (2072 under RCP8.5) Hector projects that the low latitude oceans Ω_{Ar} will drop below 3, well outside of the preindustrial values of $\Omega_{Ar} > 3.5$ and the Ω_{Ca} high latitude will drop below 2. While at the end of the 21st Century, the oceans are not undersaturated ($\Omega < 1$), the threshold for biogenic carbonate precipitation is species dependent and can be significantly higher than 1 when combined with other factors. For example, some coral reef communities need to develop in waters that have $\Omega_{Ar} > 3.3$ (Pelejero et al., 2010; Hoegh-Guldberg et al., 2007; Kleypas et al., 1999). The lowest observed Ω_{Ar} found in individual coral reef ecosystems was $\Omega_{Ar} = 2.85$ (Shamberger et al., 2011).

Figure 7 highlights the relationship between surface temperature change and surface carbonate chemistry changes across the 4 RCPs. Under RCP 8.5, for every one degree of surface warming surface in Hector (CMIP5), pH declines by 0.107 (0.122) units (change relative to 1990–1999 plotted over 2006–2100). This is similar to Bopp et al., who calculated a global change of $0.125 \text{ units } ^\circ\text{C}^{-1}$ across the CMIP5 models. Under RCP 8.5, for every one degree of surface warming surface in Hector (CMIP5), aragonite saturation declines by 0.438 (0.432) units. For calcite saturations (not shown), for every one degree of surface warming in Hector (CMIP5), calcite saturations decrease by 0.681 (0.673) units. Our high latitude ocean box warms faster than the rest of the world's oceans, therefore, we chose to combine both the high and low latitude oceans

BGD

12, 19269–19305, 2015

Projections of ocean acidification over the next three centuries

C. A. Hartin et al.

[Title Page](#)

[Abstract](#)

[Introduction](#)

[Conclusions](#)

[References](#)

[Tables](#)

[Figures](#)

◀

▶

◀

▶

[Back](#)

[Close](#)

[Full Screen / Esc](#)

[Printer-friendly Version](#)

[Interactive Discussion](#)



into one global value, also making it easier to compare to Bopp et al. (2013). This is an area of future research to better emulate the high latitude surface ocean temperature.

Lastly, Fig. 8 highlights pH and Ω_{Ar} projections under all four RCPs from 1850 to 2300. Over the last 20 years both pH and Ω_{Ar} have declined sharply and will continue to rapidly decline under RCP 4.5, 6.0 and 8.5.
5

6 Conclusions

We developed a simple, open-source, object oriented carbon cycle climate model, Hector, that reliably reproduces the median of the CMIP5 climate variables (Hartin et al., 2015). The ocean component presented in this study, directly calculates the upper 10 ocean carbonate system (pCO_2 , DIC, pH, Ω_{Ar} , Ω_{Ca}). Under all four RCPs, pH, Ω_{Ar} , and Ω_{Ca} decrease significantly outside of their preindustrial values. In the near future the open ocean and coral reef communities are likely to experience pH and carbonate saturation levels that are unprecedented in the potentially the last 2 million years (Hönisch et al., 2009). Even at a best case scenario, RCP 2.6 (Fig. 8), pH will drop to 15 7.73 by 2100 and to 7.43 by 2300. This may result in drastic changes to marine ecosystems in particular the $CaCO_3^-$ secreting organism. For example, the rate of coral reef building decreases, calcification rates of planktonic cocolithophores and foraminifera decreases, changes in trophic level interactions and ecosystems, have all been proposed to be potential consequences of ocean acidification (Cooley and Doney, 2009; 20 Silverman et al., 2009; Fabry et al., 2008; Riebesell et al., 2000).

Organic carbon, $CaCO_3$ sediment interactions, and changes in ocean circulation are not currently simulated within Hector. We assume negligible $CaCO_3$ interactions on hundred year time scales; however, this is a necessary component under interglacial and glacial cycles. We neglect any climate feedbacks on the carbon cycle resulting 25 from changes in ocean circulation. CMIP5 models show up to a 60 % decrease in the Atlantic meridional overturning circulation by 2100 (Cheng et al., 2013). While this may have a significant impact on the uptake and transport of carbon, in Hector v1.1, we

BGD

12, 19269–19305, 2015

Projections of ocean acidification over the next three centuries

C. A. Hartin et al.

[Title Page](#)

[Abstract](#)

[Introduction](#)

[Conclusions](#)

[References](#)

[Tables](#)

[Figures](#)

◀

▶

◀

▶

[Back](#)

[Close](#)

[Full Screen / Esc](#)

[Printer-friendly Version](#)

[Interactive Discussion](#)



hold ocean circulation constant with time and accurately simulate global variables out to 2100 with a slight bias after 2100. We also note that other factors such as eutrophication, river discharge, and upwelling will likely increase the probability that coastal regions will experience the effects of ocean acidification sooner than the projected open ocean values in Hector (Ekstrom et al., 2015).

This study is timely because the CMIP5 archive, includes a large suite of ESMs that contained dynamic biogeochemistry, allowing us to study future projections of the marine carbon cycle. Rather than running the earth system models, we can use Hector to quickly emulate the CMIP5 median for projection studies under different emission pathways and uncertainty analyses of the marine carbonate system. Due to Hector's simplistic nature and fast execution times, Hector has the potential to be a critical tool to the decision-making, scientific, and integrated assessment communities, allowing for further understanding of future changes to the marine carbonate system.

Appendix: Carbonate Chemistry

Modified from Zeebe and Wolf-Gladrow (2001)

$$\text{DIC}^* \left(\frac{K_1}{[\text{H}^+]} + 2 \frac{K_1 K_2}{[\text{H}^+]^2} \right) = \left(\text{TA} - \frac{K_B B_T}{K_B + [\text{H}^+]} - \frac{K_W}{[\text{H}^+]} + [\text{H}^+] \right) * \left(1 + \frac{K_1}{[\text{H}^+]} + \frac{K_1 K_2}{[\text{H}^+]^2} \right) \quad (\text{A1})$$

This equation results in a higher order polynomial equation for H^+ , in which the roots (1 positive, 4 negative) are solved for. Once H^+ is solved for, pH, $p\text{CO}_2$, HCO_3^- , and CO_3^{2-} can be determined.

$$[\text{CO}_2^*] = \frac{\text{DIC}}{\left(1 + \frac{K_1}{[\text{H}^+]} + \frac{K_1 K_2}{[\text{H}^+]^2} \right)} \quad (\text{A2})$$

$$p\text{CO}_2 = \frac{[\text{CO}_2^*]}{K_H} \quad (\text{A3})$$

[Title Page](#)

[Abstract](#)

[Introduction](#)

[Conclusions](#)

[References](#)

[Tables](#)

[Figures](#)

[◀](#)

[▶](#)

[◀](#)

[▶](#)

[Back](#)

[Close](#)

[Full Screen / Esc](#)

[Printer-friendly Version](#)

[Interactive Discussion](#)



$$[\text{HCO}_3^-] = \frac{\text{DIC}}{\left(1 + \frac{[\text{H}^+]}{K_1} + \frac{K_2}{[\text{H}^+]}\right)} \quad (\text{A4})$$

$$[\text{CO}_3^{2-}] = \frac{\text{DIC}}{\left(1 + \frac{[\text{H}^+]}{K_2} + \frac{[\text{H}^+]^2}{K_1 K_2}\right)} \quad (\text{A5})$$

$$K_1 = \frac{[\text{H}^+] [\text{HCO}_3^-]}{[\text{CO}_2]} \quad (\text{A6})$$

$$K_2 = \frac{[\text{H}^+] [\text{CO}_3^{2-}]}{[\text{HCO}_3^-]} \quad (\text{A7})$$

- ⁵ K_1 and K_2 are the first and second acidity constants of carbonic acid from Mehrbach et al. (1973) and refit by Lueker et al. (2000).

$$K_B = \frac{[\text{H}^+] [\text{B(OH)}_4^-]}{[\text{B(OH)}_3]} \quad (\text{A8})$$

K_B is the dissociation constant of boric acid from DOE (1994).

$$K_W = \frac{[\text{H}^+]}{[\text{OH}^-]} \quad (\text{A9})$$

- ¹⁰ K_W is the dissociation constant of water from Millero (1995).

$$K_{\text{sp}} = [\text{Ca}^{2+}] * [\text{CO}_3^{2-}] \quad (\text{A10})$$

K_{sp} of aragonite and calcite is calculated from Mucci, (1983).

For those equations with multiple coefficients please see the references listed below.



Title Page	Abstract	Introduction
Conclusions	References	
Tables	Figures	
◀	▶	
◀	▶	
Back	Close	
Full Screen / Esc		
Printer-friendly Version		
Interactive Discussion		

Projections of ocean acidification over the next three centuries

C. A. Hartin et al.

[Title Page](#)[Abstract](#)[Introduction](#)[Conclusions](#)[References](#)[Tables](#)[Figures](#)[◀](#)[▶](#)[◀](#)[▶](#)[Back](#)[Close](#)[Full Screen / Esc](#)[Printer-friendly Version](#)[Interactive Discussion](#)

1. K_H and K_0 are similar equations calculating Henry's constant or the solubility of CO_2 , however they return different units ($\text{mol kg}^{-1} \text{ atm}^{-1}$ and $\text{mol L}^{-1} \text{ atm}^{-1}$) (see Weiss, 1974 for equations and coefficients). K_H is used to solve $p\text{CO}_2$ while K_0 is used to solve air-sea fluxes of CO_2 .

5 2. The Schmidt number is taken from Wanninkhof (1992) for coefficients of CO_2 in seawater.

Ca (mol kg^{-1}) is calculated from Riley and Rongudai (1967)

10 *Author contributions.* C. Hartin designed and carried out the experiments. C. Hartin, B. Bond-Lamberty, and P. Patel developed the model code. A. Mundra process data, design and prepare figures. C. Hartin prepared the manuscript with contributions from all co-authors.

Acknowledgement. This research is based on work supported by the US Department of Energy. The Pacific Northwest National Laboratory is operated for DOE by Battelle Memorial Institute under contract DE-AC05-76RL01830.

References

- 15 Albright, R., Langdon, C., and Anthony, K. R. N.: Dynamics of seawater carbonate chemistry, production, and calcification of a coral reef flat, central Great Barrier Reef, Biogeosciences, 10, 6747–6758, doi:10.5194/bg-10-6747-2013, 2013.
- Bates, N. R.: Interannual variability of the oceanic CO_2 sink in the subtropical gyre of the North Atlantic Ocean over the last 2 decades, J. Geophys. Res.-Oceans, 112, C09013, doi:10.1029/2006JC003759, 2007.
- 20 Bopp, L., Resplandy, L., Orr, J. C., Doney, S. C., Dunne, J. P., Gehlen, M., Halloran, P., Heinze, C., Ilyina, T., Séférian, R., Tjiputra, J., and Vichi, M.: Multiple stressors of ocean ecosystems in the 21st century: projections with CMIP5 models, Biogeosciences Discuss., 10, 3627–3676, doi:10.5194/bgd-10-3627-2013, 2013.
- 25 Broecker, W. S. and Peng, T.: Tracers in the Sea, edited by: Lamont-Doherty Geological Observatory, Tracers in the Sea, Palisades, NY, Palisades, NY, Lamont-Doherty Geological Observatory, c1982, 1982.

Projections of ocean acidification over the next three centuries

C. A. Hartin et al.

- Byrne, R. H., Mecking, S., Feely, R. A., and Liu, X.: Direct observations of basin-wide acidification of the North Pacific Ocean, *Geophys. Res. Lett.*, 37, L02601, doi:10.1029/2009GL040999, 2010.
- Caldeira, K., Jain, A. K., and Hoffert, M. I.: Climate sensitivity uncertainty and the need for energy without CO₂ emission, *Science*, 299, 2052–2054, doi:10.1126/science.1078938, 2003.
- Cheng, W., Chiang, J. C. H., and Zhang, D.: Atlantic Meridional Overturning Circulation (AMOC) in CMIP5 Models: RCP and Historical Simulations, *J. Climate*, 26, 7187–7197, doi:10.1175/JCLI-D-12-00496.1, 2013.
- Clarke, L., J. Edmonds, H. Jacoby, H. Pitcher, Reilly, J., and Richels, R.: Scenarios of Greenhouse Gas Emissions and Atmospheric Concentrations. Sub-report 2.1A of Synthesis and Assessment Product 2.1, edited by: US Climate Change Science Program and the Subcommittee on Global Change Research, Department of Energy, Office of Biological & Environmental Research, Washington, DC, USA, 2007.
- Cooley, S. R. and Doney, S. C.: Anticipating ocean acidification's economic consequences for commercial fisheries, *Environ. Res. Lett.*, 4, 024007, doi:10.1088/1748-9326/4/2/024007, 2009.
- Copin-Montegut, C.: A new formula for the effect of temperature on the partial pressure of CO₂ in seawater, *Mar. Chem.*, 25, 29–37, doi:10.1016/0304-4203(88)90012-6, 1988.
- DOE: Handbook of Methods for the Analysis of the Various Parameters of the Carbon Dioxide System in Sea Water, edited by: Dickson, A. G., and Goyet, C., ORNL/CDIAC-74, US Dept. of Energy, 1994.
- Doney, S. C.: The growing human footprint on coastal and open-ocean biogeochemistry, *Science*, 328, 1512–1516, doi:10.1126/science.1185198, 2010.
- Dore, J. E., Lukas, R., Sadler, D. W., Church, M. J., and Karl, D. M.: Physical and biogeochemical modulation of ocean acidification in the central North Pacific, *P. Natl. Acad. Sci. USA*, 106, 12235–12240, doi:10.1073/pnas.0906044106, 2009.
- Dutkiewicz, S., Morris, J. J., Follows, M. J., Scott, J., Levitan, O., Dyhrman, S. T., and Bermann-Frank, I.: Impact of ocean acidification on the structure of future phytoplankton communities, *Nature Clim. Change*, 5, 1002–1006, doi:10.1038/nclimate2722, 2015.
- Ekstrom, J. A., Suatoni, L., Cooley, S. R., Pendleton, L. H., Waldbusser, G. G., Cinner, J. E., Ritter, J., Langdon, C., van Hoidonk, R., Gledhill, D., Wellman, K., Beck, M. W., Brander, L. M., Rittschof, D., Doherty, C., Edwards, P. E. T., and Portela, R.: Vulnerability and

Title Page	
Abstract	Introduction
Conclusions	References
Tables	Figures
◀	▶
◀	▶
Back	Close
Full Screen / Esc	
Printer-friendly Version	
Interactive Discussion	



adaptation of US shellfisheries to ocean acidification, *Nature Clim. Change*, 5, 207–214, doi:10.1038/nclimate2508, 2015.

Fabry, V. J., Seibel, B. A., Feely, R. A., and Orr, J. C.: Impacts of ocean acidification on marine fauna and ecosystem processes, *ICES Journal of Marine Science: Journal du Conseil*, 65, 414–432, doi:10.1093/icesjms/fsn048, 2008.

Feely, R. A., Sabine, C. L., Lee, K., Berelson, W., Kleypas, J., Fabry, V. J., and Millero, F. J.: Impact of anthropogenic CO₂ on the CaCO₃ system in the oceans, *Science*, 305, 362–366, doi:10.1126/science.1097329, 2004.

Feely, R. A., Doney, S. C., and Cooley, S. R.: Ocean Acidification: Present Conditions and Future Changes in a High-CO₂ World, *Oceanography*, 22, 36–47, 2009.

Feely, R. A., Sabine, C. L., Byrne, R. H., Millero, F. J., Dickson, A. G., Wanninkhof, R., Murata, A., Miller, L. A., and Greeley, D.: Decadal changes in the aragonite and calcite saturation state of the Pacific Ocean, *Global Biogeochem. Cy.*, 26, GB3001, doi:10.1029/2011GB004157, 2012.

Fujieki, L., Santiago-Mandujano, F., Fumar, C., Liukas, R., and Church, M.: Hawaii Ocean Time-series Program Data Report, School of Ocean and Earth Science and Technology, Univ. of Hawaii, Honolulu, HI, 492 pp., 2013.

Fujino, J., Nair, R., Kainuma, M., Masui, T., and Matsuoka, Y.: Multi-gas Mitigation Analysis on Stabilization Scenarios Using Aim Global Model, *The Energy Journal*, 27, 343–353, 2006.

Gehlen, M., Séférian, R., Jones, D. O. B., Roy, T., Roth, R., Barry, J., Bopp, L., Doney, S. C., Dunne, J. P., Heinze, C., Joos, F., Orr, J. C., Resplandy, L., Segschneider, J., and Tijiputra, J.: Projected pH reductions by 2100 might put deep North Atlantic biodiversity at risk, *Biogeosciences Discuss.*, 11, 8607–8634, doi:10.5194/bgd-11-8607-2014, 2014.

Harman, I. N., Trudinger, C. M., and Raupach, M. R.: SCCM – the Simple Carbon-Climate Model: Technical Documentation, Centre for Australian Weather and Climate Research, Bureau of Meteorology and CSIRO, Melbourne, Australia,, 2011.

Hartin, C. A., Patel, P., Schwarber, A., Link, R. P., and Bond-Lamberty, B. P.: A simple object-oriented and open-source model for scientific and policy analyses of the global climate system – Hector v1.0, *Geosci. Model Dev.*, 8, 939–955, doi:10.5194/gmd-8-939-2015, 2015.

Hijioka, Y., Matsuoka, Y., Nishimoto, H., Masui, M., and Kainuma, M.: Global GHG emissions scenarios under GHG concentration stabilization targets, *Journal of Environmental Engineering*, 13, 97–108, 2008.

BGD

12, 19269–19305, 2015

Projections of ocean acidification over the next three centuries

C. A. Hartin et al.

[Title Page](#)

[Abstract](#)

[Introduction](#)

[Conclusions](#)

[References](#)

[Tables](#)

[Figures](#)



[Back](#)

[Close](#)

[Full Screen / Esc](#)

[Printer-friendly Version](#)

[Interactive Discussion](#)



- Hönisch, B., Hemming, N. G., Archer, D., Siddall, M., and McManus, J. F.: Atmospheric carbon dioxide concentration across the mid-Pleistocene transition, *Science*, 324, 1551–1554, doi:10.1126/science.1171477, 2009.
- Irvine, P. J., Srivastava, R. L., and Keller, K.: Tension between reducing sea-level rise and global warming through solar-radiation management, *Nature Climate Change*, 2, 97–100, doi:10.1038/nclimate1351, 2012.
- Joos, F., Bruno, M., Fink, R., Siegenthaler, U., Stocker, T. F., Le Quéré, C., and Sarmiento, J. L.: An efficient and accurate representation of complex oceanic and biospheric models of anthropogenic carbon uptake, *Tellus B*, 48, 397–417, doi:10.1034/j.1600-0889.1996.t01-2-00006.x, 1996.
- Joos, F., Plattner, G.-K., Stocker, T. F., Marchal, O., and Schmittner, A.: Global Warming and Marine Carbon Cycle Feedbacks on Future Atmospheric CO₂, *Science*, 284, 464–467, doi:10.1126/science.284.5413.464, 1999.
- Joos, F., Prentice, I. C., Sitch, S., Meyer, R., Hooss, G., Plattner, G.-K., Gerber, S., and Hasselmann, K.: Global warming feedbacks on terrestrial carbon uptake under the Intergovernmental Panel on Climate Change (IPCC) emission scenarios, *Global Biochem. Cy.*, 15, 891–907, 2001.
- Key, R. M., Kozyr, A., Sabine, C. L., Lee, K., Wanninkhof, R., Bullister, J. L., Feely, R. A., Millero, F. J., Mordy, C., and Peng, T. H.: A global ocean carbon climatology: results from Global Data Analysis Project (GLODAP), *Global Biogeochem. Cy.*, 18, GB4031, doi:10.1029/2004GB002247, 2004.
- Kleypas, J. A., Buddemeier, R. W., Archer, D., Gattuso, J.-P., Langdon, C., and Opdyke, B. N.: Geochemical Consequences of Increased Atmospheric Carbon Dioxide on Coral Reefs, *Science*, 284, 118–120, doi:10.1126/science.284.5411.118, 1999.
- Kleypas, J. A., Feely, R. A., Fabry, V. J., Langdon, C., Sabine, C. L., and Robbins, L. L.: Impacts of ocean acidification on coral reefs and other marine calcifiers: a guide for future research, Report of a Workshop Held 18–20 April 2005, St. Petersburg, FL, Sponsored by NSF, NOAA, and the US Geological Survey, Kurihara, H., 2008.
- Knox, F. and McElroy, M. B.: Changes in Atmospheric CO₂: Influence of the Marine Biota at High Latitude, *J. Geophys. Res.*, 89, 4629–4637, doi:10.1029/JD089iD03p04629, 1984.
- Kump, L. R., Bralower, T. R., and Ridgwell, A. J.: Ocean acidification in deep time, *Oceanography*, 22, 94–107, 2009.

Projections of ocean acidification over the next three centuries

C. A. Hartin et al.

[Title Page](#)[Abstract](#)[Introduction](#)[Conclusions](#)[References](#)[Tables](#)[Figures](#)[◀](#)[▶](#)[◀](#)[▶](#)[Back](#)[Close](#)[Full Screen / Esc](#)[Printer-friendly Version](#)[Interactive Discussion](#)

- Le Quéré, C., Rödenbeck, C., Buitenhuis, E. T., Conway, T. J., Langenfelds, R., Gomez, A., Labuschagne, C., Ramonet, M., Nakazawa, T., Metzl, N., Gillett, N., and Heimann, M.: Saturation of the Southern Ocean CO₂ sink due to recent climate change, *Science*, 316, 1735–1738, doi:10.1126/science.1136188, 2007.
- 5 Le Quéré, C., Takahashi, T., Buitenhuis, E. T., Rödenbeck, C., and Sutherland, S. C.: Impact of climate change and variability on the global oceanic sink of CO₂, *Global Biogeochem. Cy.*, 24, GB4007, doi:10.1029/2009GB003599, 2010.
- 10 Le Quéré, C., Andres, R. J., Boden, T., Conway, T., Houghton, R. A., House, J. I., Marland, G., Peters, G. P., van der Werf, G. R., Ahlström, A., Andrew, R. M., Bopp, L., Canadell, J. G., Ciais, P., Doney, S. C., Enright, C., Friedlingstein, P., Huntingford, C., Jain, A. K., Jourdain, C., Kato, E., Keeling, R. F., Klein Goldewijk, K., Levis, S., Levy, P., Lomas, M., Poulter, B., Rau-pach, M. R., Schwinger, J., Sitch, S., Stocker, B. D., Viovy, N., Zaehle, S., and Zeng, N.: The global carbon budget 1959–2011, *Earth Syst. Sci. Data*, 5, 165–185, doi:10.5194/essd-5-165-2013, 2013.
- 15 Lenton, T. M.: Land and ocean carbon cycle feedback effects on global warming in a simple earth system model, *Tellus B*, 52, 1159–1188, doi:10.1034/j.1600-0889.2000.01104.x, 2000.
- Lueker, T. J., Dickson, A. G., and Keeling, C. D.: Ocean pCO₂ calculated from dissolved inorganic carbon, alkalinity, and equations for K1 and K2; validation based on laboratory measurements of CO₂ in gas and seawater at equilibrium, *Mar. Chem.*, 70, 105–119, 2000.
- 20 Matear, R. J. and Hirst, A. C.: Climate change feedback on the future oceanic CO₂ uptake, *Tellus B*, 51, 722–733, doi:10.1034/j.1600-0889.1999.t01-1-00012.x, 1999.
- Mehrback, C., Culberson, C. H., Hawley, J. E., and Pytkowicz, R. M.: Measurement of the apparent dissociation constants of carbonic acid in seawater at atmospheric pressure, *Limnol. Oceanogr.*, 18, 897–907, 1973.
- 25 Meinshausen, M., Raper, S. C. B., and Wigley, T. M. L.: Emulating coupled atmosphere-ocean and carbon cycle models with a simpler model, MAGICC6 – Part 1: Model description and calibration, *Atmos. Chem. Phys.*, 11, 1417–1456, doi:10.5194/acp-11-1417-2011, 2011.
- Millero, F. J.: Thermodynamics of the carbon dioxide system in the oceans, *Geochim. Cosmochim. Ac.*, 59, 661–677, doi:10.1016/0016-7037(94)00354-O, 1995.
- 30 Montenegro, A., Brovkin, V., Eby, M., Archer, D., and Weaver, A. J.: Long term fate of anthropogenic carbon, *Geophys. Res. Lett.*, 34, 2007.
- Moss, R. H., Edmonds, J. A., Hibbard, K. A., Manning, M. R., Rose, S. K., van Vuuren, D. P., Carter, T. R., Emori, S., Kainuma, M., Kram, T., Meehl, G. A., Mitchell, J. F. B., Nakai,

Projections of ocean acidification over the next three centuries

C. A. Hartin et al.

[Title Page](#)

[Abstract](#)

[Introduction](#)

[Conclusions](#)

[References](#)

[Tables](#)

[Figures](#)

◀

▶

◀

▶

[Back](#)

[Close](#)

[Full Screen / Esc](#)

[Printer-friendly Version](#)

[Interactive Discussion](#)



cenovic, N., Riahi, K., Smith, S. J., Stouffer, R. J., Thomson, A. M., Weyant, J. P., and Wilbanks, T. J.: The next generation of scenarios for climate change research and assessment, *Nature*, 463, 747–756, doi:10.1038/nature08823, 2010.

Mucci, A.: The solubility of calcite and aragonite in seawater at various salinities, temperatures
5 and at one atmosphere pressure, *Amer. J. of Science*, 283, 781–799, 1983.

Orr, J. C., Fabry, V. J., Aumont, O., Bopp, L., Doney, S. C., Feely, R. A., Gnanadesikan, A., Gruber, N., Ishida, A., Joos, F., Key, R. M., Lindsay, K., Maier-Reimer, E., Matear, R., Monfray, P., Mouchet, A., Najjar, R. G., Plattner, G.-K., Rodgers, K. B., Sabine, C. L., Sarmiento, J. L., Schlitzer, R., Slater, R. D., Totterdell, I. J., Weirig, M.-F., Yamanaka, Y., and Yool, A.: Anthropogenic ocean acidification over the twenty-first century and its impact on calcifying organisms, *Nature*, 437, 681–686, doi:10.1038/nature04095, 2005.

Pelejero, C., Calvo, E., McCulloch, M. T., Marshall, J. F., Gagan, M. K., Lough, J. M., and Opdyke, B. N.: Preindustrial to Modern Interdecadal Variability in Coral Reef pH, *Science*, 309, 2204–2207, doi:10.1126/science.1113692, 2005.

15 Pietsch, S. A. and Hasenauer, H.: Evaluatin the self-initialization procedure for large-scale ecosystem models., *Glob. Change Biol.*, 12, 1–12, 2006.

Raven, J., Caldeira, K., Elderfield, H., Hoegh-Guldberg, O., Liss, P., Riebesell, U., Shepherd, J., Turley, C., and Watson, A.: Ocean Acidification Due To Increasing Atmospheric Carbon Dioxide, The Royal Society, Cardiff, UK, 2005.

20 Riahi, K., Grubler, A., and Nakicenovic, N.: Scenarios of long-term socio-economic and environmental development under climate stabilization, *Technol. Forecast. Soc.*, 74, 887–935, 2007.

Riahi, K., Rao, S., Krey, V., Cho, C., Chirkov, V., Fischer, G., Kindermann, G., Nakicenovic, N., and Rafaj, P.: RCP 8.5 – A scenario of comparatively high greenhouse gas emissions, *Climatic Change*, 109, 33–57, doi:10.1007/s10584-011-0149-y, 2011.

Ricciuto, D. M., Davis, K. J., and Keller, K.: A Bayesian calibration of a simple carbon cycle model: the role of observations in estimating and reducing uncertainty, *Global Biogeochem. Cy.*, 22, GB2030, doi:10.1029/2006GB002908, 2008.

30 Ricke, K. L., Orr, J. C., Schneider, K., and Caldeira, K.: Risks to coral reefs from ocean carbonate chemistry changes in recent earth system model projections, *Environ. Res. Lett.*, 8, 034003, doi:10.1088/1748-9326/8/3/034003, 2013.

BGD

12, 19269–19305, 2015

Projections of ocean acidification over the next three centuries

C. A. Hartin et al.

Title Page

Abstract

Introduction

Conclusions

References

Tables

Figures



Back

Close

Full Screen / Esc

Printer-friendly Version

Interactive Discussion



- Riebesell, U., Zondervan, I., Rost, B., Tortell, P. D., Zeebe, R. E., and Morel, F. M. M.: Reduced calcification of marine plankton in response to increased atmospheric CO₂, *Nature*, 407, 364–367, 2000.
- Riley, J. P. and Tongudai, M.: The major cation/chlorinity ratios in sea water, *Chem. Geol.*, 2, 263–269, doi:10.1016/0009-2541(67)90026-5, 1967.
- Sabine, C. L., Feely, R. A., Gruber, N., Key, R. M., Lee, K., Bullister, J. L., Wanninkhof, R., Wong, C. S., Wallace, D. W. R., Tilbrook, B., Millero, F. J., Peng, T.-H., Kozyr, A., Ono, T., and Rios, A. F.: The oceanic sink for anthropogenic CO₂, *Science*, 305, 367–371, doi:10.1126/science.1097403, 2004.
- Sabine, C. L., Feely, R., Wanninkhof, R., Takahashi, T., Khatiwala, S., and Park, G.-H.: The global ocean carbon cycle, In *State of the Climate in 2010*, 3, Global Oceans, B. Am. Meteorol. Soc., 92, S100–S108, doi:10.1175/1520-0477-92.6.S1, 2011.
- Santana-Casiano, J. M., González-Dávila, M., Rueda, M.-J., Llinás, O., and González-Dávila, E.-F.: The interannual variability of oceanic CO₂ parameters in the northeast Atlantic subtropical gyre at the ESTOC site, *Global Biogeochem. Cy.*, 21, GB1015, doi:10.1029/2006GB002788, 2007.
- Sarmiento, J. L. and Le Quéré, C.: Oceanic carbon dioxide uptake in a model of century-scale global warming, *Science*, 274, 1346–1350, doi:10.1126/science.274.5291.1346, 1996.
- Sarmiento, J. L. and Toggweiler, J. R.: A new model for the role of the oceans in determining atmospheric pCO₂, *Nature*, 308, 621–624, 1984.
- Senior, C. A. and Mitchell, J. F. B.: The time-dependence of climate sensitivity, *Geophys. Res. Lett.*, 27, 2685–2688, doi:10.1029/2000GL011373, 2000.
- Shamberger, K. E. F., Feely, R. A., Sabine, C. L., Atkinson, M. J., DeCarlo, E. H., Mackenzie, F. T., Drupp, P. S., and Butterfield, D. A.: Calcification and organic production on a Hawaiian coral reef, *Mar. Chem.*, 127, 64–75, doi:10.1016/j.marchem.2011.08.003, 2011.
- Siegenthaler, U. and Joos, F.: Use of a simple model for studying oceanic tracer distributions and the global carbon cycle, *Tellus B*, 44, 186–207, doi:10.1034/j.1600-0889.1992.t01-2-00003.x, 1992.
- Silverman, J., Lazar, B., Cao, L., Caldeira, K., and Erez, J.: Coral reefs may start dissolving when atmospheric CO₂ doubles, *Geophys. Res. Lett.*, 36, doi:10.1029/2008GL036282, 2009.
- Smith, S. and Wigley, T.: Multi-Gas Forcing Stabilization with the MiniCAM, *Energ. J.*, Special Issue #3, 373–391, 2006.

Title Page	
Abstract	Introduction
Conclusions	References
Tables	Figures
◀	▶
◀	▶
Back	Close
Full Screen / Esc	
Printer-friendly Version	
Interactive Discussion	



- Takahashi, T., Olafsson, J., Goddard, J. G., Chipman, D. W., and Sutherland, S. C.: Seasonal variation of CO₂ and nutrients in the high-latitude surface oceans: a comparative study, *Global Biogeochem. Cy.*, 7, 843–878, doi:10.1029/93GB02263, 1993.
- Takahashi, T., Sutherland, S. C., Wanninkhof, R., Sweeney, C., Feely, R. A., Chipman, D. W., Hales, B., Friederich, G., Chavez, F., Sabine, C., Watson, A., Bakker, D. C. E., Schuster, U., Metzl, N., Yoshikawa-Inoue, H., Ishii, M., Midorikawa, T., Nojiri, Y., Körtzinger, A., Steinhoff, T., Hoppema, M., Olafsson, J., Arnarson, T. S., Tilbrook, B., Johannessen, T., Olsen, A., Bellerby, R., Wong, C. S., Delille, B., Bates, N. R., and de Baar, H. J. W.: Climatological mean and decadal change in surface ocean pCO₂, and net sea-air CO₂ flux over the global oceans, *Deep-Sea Res. Pt. II*, 56, 554–577, doi:10.1016/j.dsrr.2008.12.009, 2009.
- Tanaka, K., Kriegler, E., Bruckner, T., Hooss, G., Knorr, W., Raddatz, T. J., and Tol, R.: Aggregated carbon cycle, atmospheric chemistry, and climate model (ACC2), Max Planck Institute, Hamburg, 1–188, 2007.
- Taylor, K. E., Stouffer, R. J., and Meehl, G. A.: An Overview of CMIP5 and the Experiment Design, *B. Am. Meteorol. Soc.*, 93, 485–498, doi:10.1175/BAMS-D-11-00094.1, 2012.
- van Vuuren, D., Elzen, M. J., Lucas, P., Eickhout, B., Strengers, B., Ruijven, B., Wonink, S., and Houdt, R.: Stabilizing greenhouse gas concentrations at low levels: an assessment of reduction strategies and costs, *Climatic Change*, 81, 119–159, doi:10.1007/s10584-006-9172-9, 2007.
- Wanninkhof, R.: Relationship between wind speed and gas exchange over the ocean, *J. Geophys. Res.: Oceans*, 97, 7373–7382, doi:10.1029/92JC00188, 1992.
- Weiss, R. F.: Carbon dioxide in water and seawater: the solubility of a non-ideal gas, *Mar. Chem.*, 2, 203–215, doi:10.1016/0304-4203(74)90015-2, 1974.
- Wise, M., Calvin, K., Thomson, A., Clarke, L., Bond-Lamberty, B., Sands, R., Smith, S. J., Janetos, A., and Edmonds, J.: Implications of Limiting CO₂ Concentrations for Land Use and Energy, *Science*, 324, 1183–1186, doi:10.1126/science.1168475, 2009.
- K. K. Yates and R. B. Halley: CO₃²⁻ concentration and pCO₂ thresholds for calcification and dissolution on the Molokai reef flat, Hawaii, *Biogeosciences Discuss.*, 3, 123–154, doi:10.5194/bgd-3-123-2006, 2006.
- Zeebe, R. E. and Wolf-Gladrow, D.: CO₂ in Seawater: Equilibrium, Kinetics, Isotopes, Elsevier, Amsterdam, 2001.

Title Page	
Abstract	Introduction
Conclusions	References
Tables	Figures
	
	
Full Screen / Esc	
Printer-friendly Version	
Interactive Discussion	



Table 1. Description and values of ocean parameters constant in Hector.

Model Parameter	Description	Value	Value
ocean_area	Area of ocean	$3.6 \times 10^{-14} \text{ m}^2$	Knox and McElroy (1984)
part_high	Fractional area of HL	0.15	Sarmiento and Toggweiler (1984)
part_low	Fractional area of LL	0.85	Sarmiento and Toggweiler (1984)
thick_HL thick_LL	Thickness of surface ocean	100 m	Knox and McElroy (1984)
thick_inter	Thickness of intermediate ocean	900 m	
thick_deep	Thickness of deep ocean	2677 m	Total depth 3777 m
HL_volume	Volume of HL	$5.4 \times 10^{-15} \text{ m}^3$	
LL_volume	Volume of LL	$3.06 \times 10^{-16} \text{ m}^3$	
I_volume	Volume of IO	$3.24 \times 10^{-17} \text{ m}^3$	
D_volume	Volume of DO	$9.64 \times 10^{-17} \text{ m}^3$	
A _s	Surface Area of HL	$5.4 \times 10^{-13} \text{ m}^2$	
A _s	Surface Area of LL	$3.06 \times 10^{-14} \text{ m}^2$	
S	Salinity HL and LL	34.5	
U	Wind speed HL and LL	6.7 ms^{-1}	

- [Title Page](#)
- [Abstract](#) | [Introduction](#)
- [Conclusions](#) | [References](#)
- [Tables](#) | [Figures](#)
- [◀](#) | [▶](#)
- [◀](#) | [▶](#)
- [Back](#) | [Close](#)
- [Full Screen / Esc](#)
- [Printer-friendly Version](#)
- [Interactive Discussion](#)



Projections of ocean acidification over the next three centuries

C. A. Hartin et al.

[Title Page](#)

[Abstract](#)

[Introduction](#)

[Conclusions](#)

[References](#)

[Tables](#)

[Figures](#)

[◀](#)

[▶](#)

[◀](#)

[▶](#)

[Back](#)

[Close](#)

[Full Screen / Esc](#)

[Printer-friendly Version](#)

[Interactive Discussion](#)



Table 2. Initial model conditions prior to the spinup phase. Carbon values change slightly after spinning up to a steady state.

Model Parameter	Description	Initial Value	Notes
T_{HL}	Temperature of high latitude surface ocean box	2°C	Lenton (2000)
T_{LL}	Temperature of low latitude surface ocean box	22°C	Lenton (2000)
C_{HL}	High Latitude carbon	140 Pg C	Lenton (2000)
C_{LL}	Low Latitude carbon	770 Pg C	Lenton (2000)
C_{IO}	Intermediate Ocean carbon	8400 Pg C	Lenton (2000)
C_{DO}	Carbon DO	26 000 Pg C	Lenton (2000)
	Preindustrial carbon flux HL	1.0 PgCyr ⁻¹	
	Preindustrial carbon flux LL	-1.0 PgCyr ⁻¹	
aT_H	High-latitude circulation	4.9e7 m ³ s ⁻¹	Tuned to give ~ 100 Pg C from surface to deep
aT_T	Thermohaline circulation	7.2e7 m ³ s ⁻¹	Tuned to give ~ 100 Pg C from surface to deep
${}^aE_{ID}$	Water mass exchange – intermediate to deep	1.25e7 m ³ s ⁻¹	Lenton (2000); Knox and McElroy (1984)
${}^aE_{LI}$	Water mass exchange – low latitude to intermediate	2.0e8 m ³ s ⁻¹	Lenton (2000); Knox and McElroy (1984)
F_L	Total Atmosphere–Land Carbon Flux	0 PgCyr ⁻¹	
F_O	Total Atmosphere–Ocean Carbon Flux	0 PgCyr ⁻¹	
tAlk_HL	Alkalinity high latitude surface	2311.0 mol kg ⁻¹	Calculated with DIC resulting in preindustrial carbon flux of 1.0 PgC
tAlk_LL	Alkalinity low latitude surface	2435.0 mol kg ⁻¹	Calculated with DIC resulting in preindustrial carbon flux of -1.0 PgC

^t solved for after spinup and then remains constant. ^a represents those parameters found within the input file.

Projections of ocean acidification over the next three centuries

C. A. Hartin et al.

Table 3. Time-series information and carbonate parameters from each location.

Time-Series Site	Location	Time-Series Length	Reference	Ocean Carbon Measurements	Data Access
BATS HOT	Sargasso Sea North Pacific	1988–2011 1988–2011	Bates (2007) Dore et al. (2007)	TA, DIC TA, DIC, pH, ρCO_2 , Ω_{Ar} , Ω_{Ca}	http://www.bios.edu/research/projects/bats http://hahana.soest.hawaii.edu/hot/hot_jgofs.html
ESTOC Iceland Sea	Canary Islands Iceland Sea	1995–2009 1985–2013	Gonzalez-Davila (2009) Olafsson (2007a)	TA, pH, ρCO_2 DIC, ρCO_2	http://www.eurosites.info/estoc.php http://cdiac.ornl.gov/oceans/Moorings/Iceland_Sea.html
Irminger Sea	Irminger Sea	1983–2013	Olafsson (2007b)	DIC, ρCO_2	http://cdiac.ornl.gov/oceans/Moorings/Irminger_Sea.html
Flinders Reef	Coral Sea	1708–1988	Pelejero et al. (2005)	pH, Ω_{Ar}	ftp://ftp.ncdc.noaa.gov/pub/data/paleo/coral/west_pacific/great_barrier/flinders2005.txt



Table 4. CMIP5 ESM models used in this study, containing ocean carbonate parameters. Note, not all variables are reported for each model under all scenarios.

Model	Model Name	Institute
CanESM2	Second Generation Canadian Earth System Model	Canadian Center for Climate Modeling and Analysis, BC, Canada
CESM1-BGC	Community Earth System Model version 1, Biogeochemistry	The National Center for Atmospheric Research and University Corporation for Atmospheric Research, United States
CNRM-CM5	National Center for Meteorological Research Climate Model version 5	National Centre for Meteorological Research and Centre Européen de Recherche et de Formation Avancée, Toulouse, France
GFDL-ESM2G	Geophysical Fluid Dynamic Laboratory Earth System Model with GOLD ocean component	Geophysical Fluid Dynamics Laboratory, United States
GFDL-ESM2M	Geophysical Fluid Dynamic Laboratory Earth System Model with MOM ocean component	Geophysical Fluid Dynamics Laboratory, United States
HadGEM2-CC	Hadley Centre Global Environmental Model, version 2 (Carbon Cycle)	Met Office Hadley Centre, UK
HadGEM2-ES	Hadley Centre Global Environmental Model, version 2 (Earth System)	Met Office Hadley Centre, UK
IPSL-CM5A-LR	L'Institut Pierre-Simon Laplace Coupled Model, version 5A, low resolution	Institut Pierre Simon Laplace, France
IPSL-CM5A-MR	L'Institut Pierre-Simon Laplace Coupled Model, version 5A, medium resolution	Institut Pierre Simon Laplace, France
IPSL-CM5B-LR	L'Institut Pierre-Simon Laplace Coupled Model, version 5A, new atmospherical physic at low resolution	Institut Pierre Simon Laplace, France
MIROC-ESM	Model for Interdisciplinary Research on Climate, Earth System Model	Atmosphere and Ocean Research Institute (The University of Tokyo), National Institute for Environmental Studies, and Japan Agency for Marine-Earth Science and Technology
MIROC-ESM-CHEM	Model for Interdisciplinary Research on Climate, Earth System Model, with atmospheric chemistry model	Atmosphere and Ocean Research Institute (The University of Tokyo), National Institute for Environmental Studies, and Japan Agency for Marine-Earth Science and Technology
MPI-ESM-LR	Max Planck Institute Earth System Model, low resolution	Max Planck Institute for Meteorology, Germany
MPI-ESM-MR	Max Planck Institute Earth System Model, medium resolution	Max Planck Institute for Meteorology, Germany
NorESM1-ME	Norwegian Earth System Model, version 1, intermediate resolution	Norwegian Climate Center, Norway

Projections of ocean acidification over the next three centuries

C. A. Hartin et al.

Table 5. Absolute values and rates of change per year (Δ) for the low (high) latitude surface ocean between 1850, 2100 and 2300 under RCP 8.5 for DIC ($\mu\text{mol kg}^{-1}$), $p\text{CO}_2$ (μatm), pH (unitless), Ω_{Ar} (unitless) and Ω_{Ca} (unitless).

DIC 1850	2100	2300	1850	$p\text{CO}_2$ 2100	2300	1850	pH 2100	2300	1850	Ω_{Ar} 2100	2300	1850	Ω_{Ar} 2100	2300	
Hector	2073.9 (2107.5)	2284.1 (2258.1)	2357.6 (2335.5)	294.7 (244.7)	879.6 (816.6)	1766.5 (1732.1)	8.17 (8.23)	7.77 (7.76)	7.50 (7.46)	4.06 (2.17)	2.21 (0.96)	1.42 (0.56)	6.22 (3.45)	3.34 (1.52)	2.13 (0.88)
Δ	1.27 (1.00)	0.47 (0.39)	3.90 (3.81)	4.43 (4.58)	-0.0027 (-0.0030)	-0.0014 (-0.0015)	-0.0123 (-0.0081)	-0.0040 (-0.0020)	-0.0192 (-0.0129)	-0.0061 (-0.0032)	-	-	-	-	-
CMIP5	2025.10 (2089.93)	2210.90 (2218.02)	2318.72 (2285.76)	292.01 (275.02)	930.87 (889.58)	1966.53 (1927.00)	8.15 (8.15)	7.73 (7.69)	7.43 (7.37)	3.56 (1.70)	1.87 (0.73)	1.21 (0.41)	5.47 (2.71)	2.84 (1.16)	1.82 (0.65)
Δ	1.24 (0.85)	0.54 (0.34)	4.26 (4.10)	5.18 (5.19)	-0.0023 (-0.0031)	-0.0015 (-0.0016)	-0.0113 (-0.0065)	-0.0033 (-0.0016)	-0.0175 (-0.0103)	-0.0051 (-0.0026)	-	-	-	-	-
Historical rates of change 1991–2011 (20 years) ^a															
BATS	DIC	$p\text{CO}_2$	pH	Ω_{Ar}	Ω_{Ca}										
BATS	1.12	2.13	-0.0022	-0.009	-0.014										
HOT	1.67	1.71	-0.0016	-0.009	-0.014										
ESTOC	1.44	0.081	-0.0025	-	-										
Iceland Sea	1.88	1.12	-0.0012	-0.006	-0.009										
Irminger Sea	1.10	1.6	-0.0023	-0.009	-0.013										
Hector	0.90	1.80	-0.0018	-0.009	-0.014										
	(0.76)	(2.88)	(-0.0021)	(-0.007)	(-0.010)										
CMIP5	1.59	1.76	-0.0017	-0.0073	-0.011										
	(2.46)	(1.45)	(-0.0028)	(-0.0054)	(-0.0089)										

Common year range across all variables for BATS, HOT, Iceland and Irminger. ESTOC is from 1995–2002

Title Page

Abstract

Introduction

Conclusions

References

Tables

Figures

◀

▶

◀

▶

Back

Close

Full Screen / Esc

Printer-friendly Version

Interactive Discussion



Projections of ocean acidification over the next three centuries

C. A. Hartin et al.

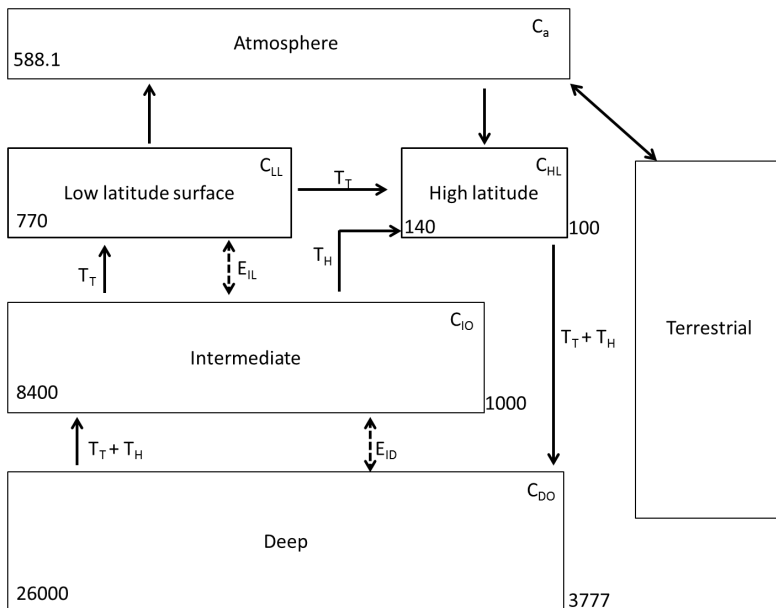


Figure 1. Representation of the steady state ocean carbon cycle in Hector. For details on the terrestrial component see Hartin et al. (2015). The atmosphere consists of one well-mixed box, connected to the surface ocean via air-sea fluxes of carbon. The ocean consists of four boxes, with advection (represented by solid arrows) and water mass exchange (represented by dashed arrows) simulating thermohaline circulation (see Table 2 for description of parameters). The carbon exchange from the high latitude to deep box is initially tuned to $\sim 100 \text{ Pg C yr}^{-1}$. The inorganic carbon cycle is solved for in the high and low latitude surface boxes. At steady state, there is a flux of carbon from the atmosphere to the high latitude surface box, while the low-latitude surface ocean releases carbon to the atmosphere. The lower left number represents the initial carbon pools of each box in Pg C yr^{-1} and the lower right hand numbers are the depth of each box in meters.

Title Page

Abstract

Introduction

Conclusions

References

Tables

Figures

1

1

1

ANSWER

Full Screen / Esc

[Printer-friendly Version](#)

Interactive Discussion



Projections of ocean acidification over the next three centuries

C. A. Hartin et al.

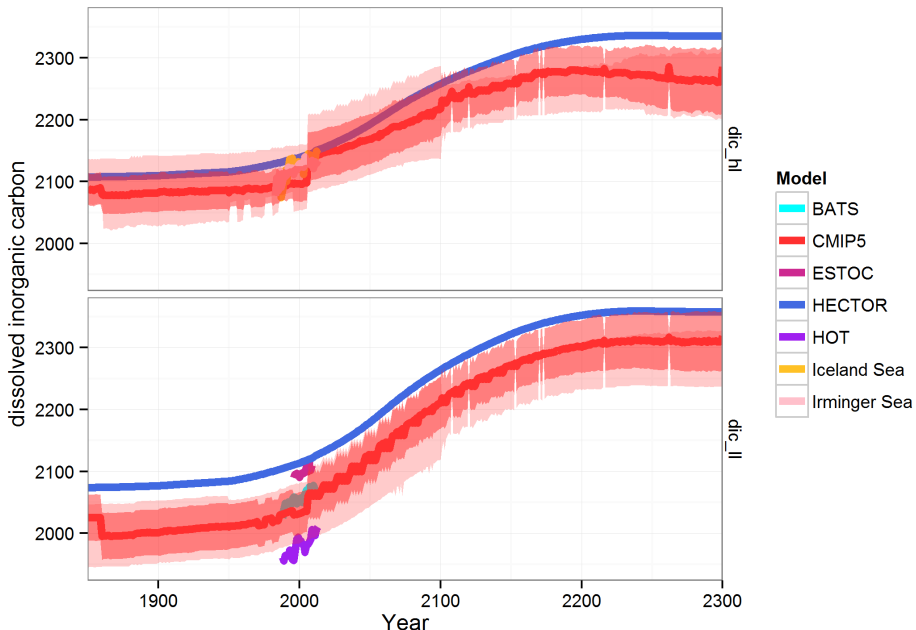


Figure 2. Dissolved inorganic carbon (DIC) for high (top) and low latitude (bottom) surface ocean under RCP 8.5; Hector (blue), CMIP5 median, standard deviation, and model range (red, $n = 13$ (1850–2100) and $n = 3$ (2101–2300)); and observations from BATS (teal), ESTOC (pink), HOT (purple), Iceland (yellow) and Irminger Sea (light pink). Note a doubling of CO_2 , from preindustrial values occurs around 2050.

19299

 CC BY

[Printer-friendly Version](#)

Interactive Discussion

[Back](#) [Close](#)

◀

Abstract

Abstract Introduction

Conclusions | References

Conclusions References

Tables

Tables

Projections of ocean acidification over the next three centuries

C. A. Hartin et al.

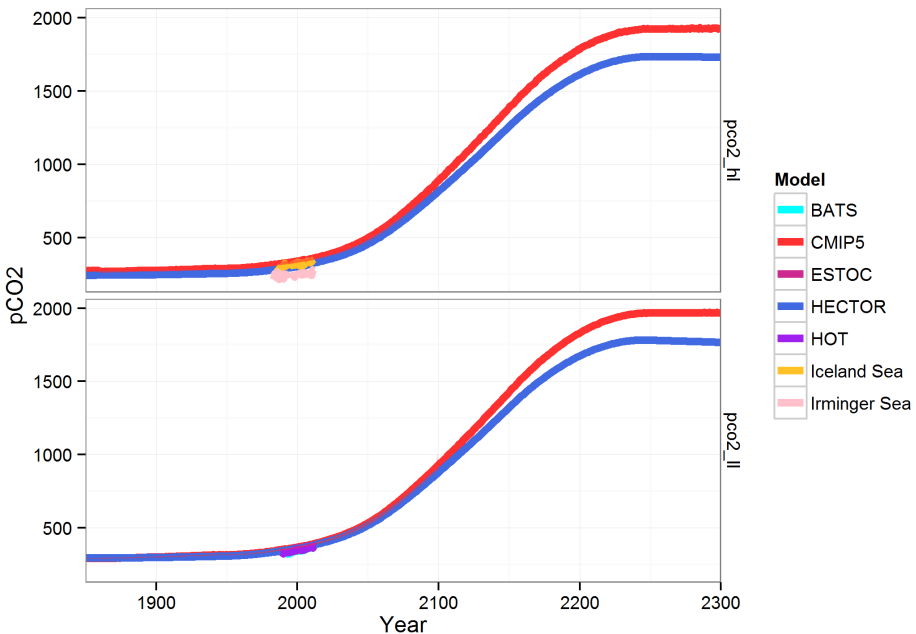


Figure 3. $p\text{CO}_2$ for high (top) and low latitude (bottom) surface ocean under RCP 8.5; Hector (blue), CMIP5 median, standard deviation, and model range (red, $n = 10$ (1850–2100) and $n = 2$ (2101–2300)); and observations from BATS (teal), HOT (purple), ESTOC (pink), Iceland (yellow) and Irminger Sea (light pink).

19300

Projections of ocean acidification over the next three centuries

C. A. Hartin et al.

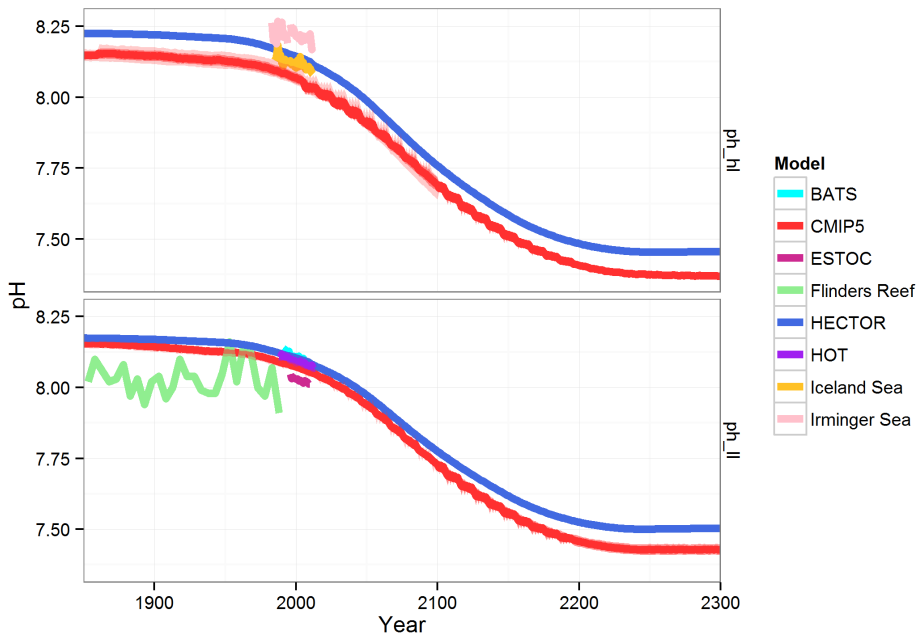


Figure 4. pH for high (top) and low latitude (bottom) surface ocean under RCP 8.5; Hector (blue), CMIP5 median, standard deviation, and model range (red, $n = 12$ (1850–2100) and $n = 2$ (2101–2300)); and observations from BATS (teal), ESTOC (pink), HOT (purple) Flinder's Reef (green), Iceland (yellow) and Irminger Sea (light pink).

19301

Projections of ocean acidification over the next three centuries

C. A. Hartin et al.

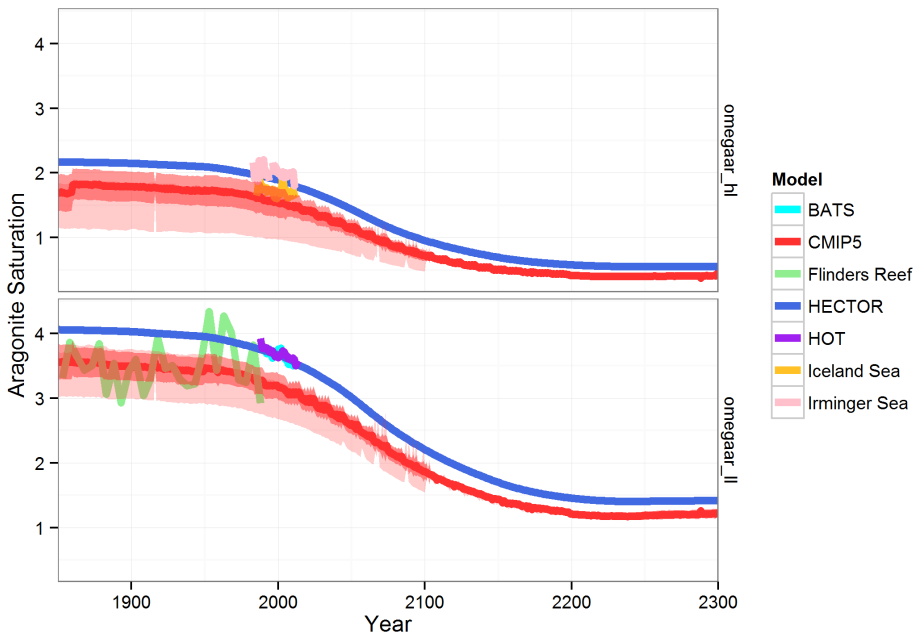


Figure 5. Aragonite saturation (Ω_{Ar}) for high (top) and low latitude (bottom) surface ocean under RCP 8.5; Hector (blue), CMIP5 median, standard deviation, and model range (red, $n = 11$ (1850–2100) and $n = 3$ (2101–2300)); and observations from BATS (teal), HOT (purple) and Flinder's Reef (green).

19302

Projections of ocean acidification over the next three centuries

C. A. Hartin et al.

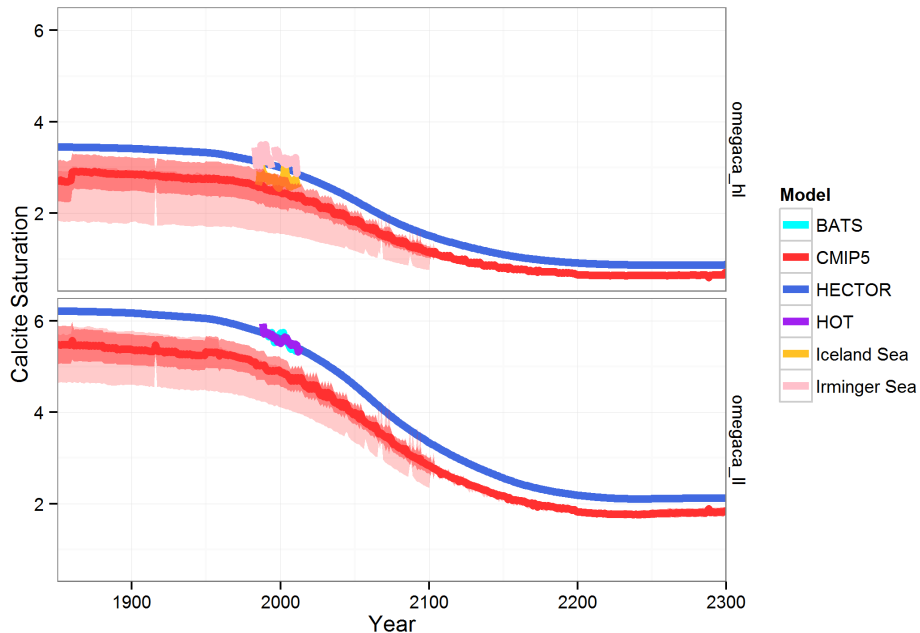


Figure 6. Calcite saturation (Ω_{Ca}) for high (top) and low latitude (bottom) surface ocean under RCP 8.5; Hector (blue), CMIP5 median, standard deviation, and model range (red, $n = 11$ (1850–2100) and $n = 3$ (2101–2300)); and observations from BATS (teal), HOT (purple), Iceland (yellow) and Irminger Sea (light pink).

Projections of ocean acidification over the next three centuries

C. A. Hartin et al.

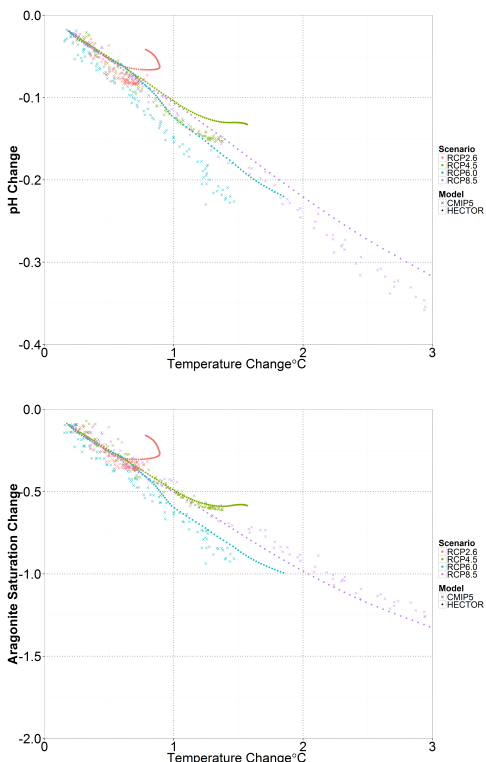


Figure 7. Relationships between the global mean change in surface pH and surface aragonite saturation, and sea surface temperature change ($^{\circ}\text{C}$) for all scenarios. These changes are relative to 1990–1999 and plotted over 2006–2100.

19304

Projections of ocean acidification over the next three centuries

C. A. Hartin et al.

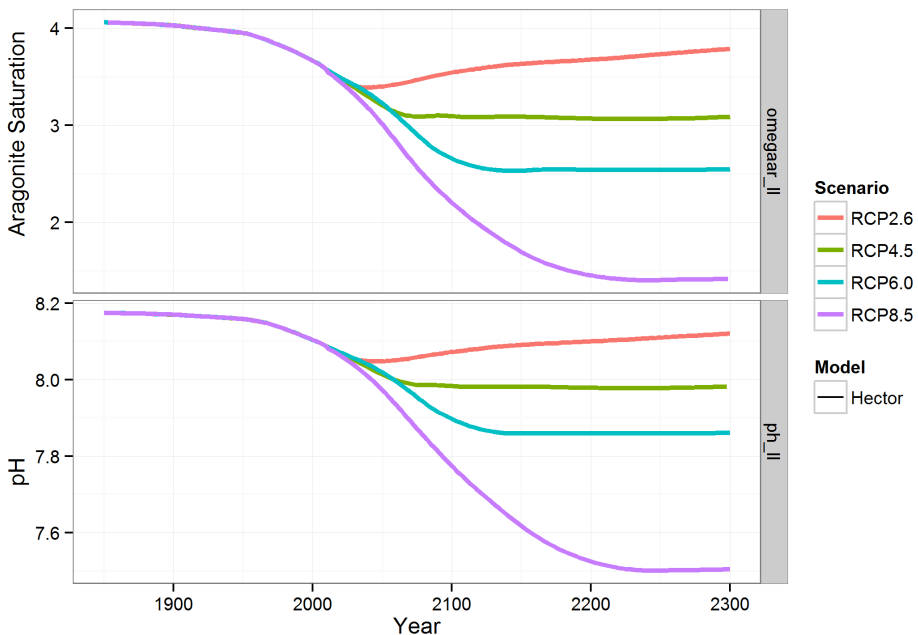


Figure 8. Low latitude aragonite saturation (Ω_{Ar}) and pH time series for Hector from 1850–2300 for RCP 2.6 (red), RCP 4.5 (green), RCP 6.0 (teal) and RCP 8.5 (purple). Note that even under a strongly mitigated scenario (RCP 2.6), both Ω_{Ar} and pH at 2300 are still lower than preindustrial values.